Comparison of D-Region Absorption During Solar Cycle 24

Michael A. Danielides (1) and Jaroslav Chum (2)

(1) Danielides Space Science Consulting (DSSC), Germany, (michael@danielides.com),
(2) Institute of Atmospheric Physics, Czech Academy of Sciences, Czech Republic (jachu@ufa.cas.cz)

Abstract:

Earth's ionosphere is formed mainly due to solar radiation, precipitating particles and cosmic rays. Its behavior is directly dependent on solar variation and the change of solar activity through out each solar cycle. The solar activity is measured by the number of sunspots and the solar radiation flux expressed by the F10.7 index. The earlier variation in electron density from solar cycle maximum to solar cycle minimum has been noted by Hargreaves (1992). He utilized the F10.7 index as a proxy for Lyman-α radiation flux, which ionizes at D-region heights mainly NO. Utilizing the IRI model the atmospheric densities of O_2^+ and N_2^+ are assumed to be constant, NO^+ density is the unknown. Also, it is known that the ionospheric reflection height depends on, e.g. diurnal variations [Pal & Chakrabarti, 2010] and other sudden ionospheric disturbances. Its longer term variations are not well enough studied.
Utilizing passive VLF ground based measurements with data coverage for almost the entire solar cycle 24, we compare solar quiet absorption curves fitted by a cosine dependence. This cosine dependence includes fixed parameters based on geography and setup of the instrument. The variables are only the solar zenith angle and the D-region absorption. This approach offers an indirect factor of NO^+ density change.
For the present study we utilize VLF monitors, which is located in northern Germany. Solar F10.7 radiation fluxes, Lyman-α radiation flux and solar X-ray radiation the Kp-Index are considered for this first comparison .
The aim of this study is a comparison of solar quiet VLF curves of the solar cycle 24 maximum and minimum. Beside the change of NO^+ density, also the variation of height of the D-region reflective layer will be discussed.

An Introduction to the Experiment

Very long frequency (VLF) radio wave propagation can be used as a tool to monitor variation of ionospheric conditions. Nowadays, VLF radio communication is still used for long distance maritime communication. There are various transmitters sending continuously signals. In this study we utilize transmissions from Cutler, Main, USA and Skelton, UK. Recording the strength of those transmissions by broad-band radio receivers provides typical disturbed night time and quiet day time curves. The receiver station is located in Mecklenburg-Lower Pommerania, Germany. In the absence of sunlight the night time ionospheric D-region – at mid latitudes - is due to the missing production of ions almost depleted and for our study not interesting. However, the undisturbed day time ionosphere provides due to photoionization a typical D-region between the height of 70 to 90 km. Additional solar events, such as intense ultraviolet and x-ray radiation events, can cause, due to enhanced photoionization, an increase in density over the entire day-side. Such ionospheric disturbances are influencing VLF radio propagation and are seen as so called sudden ionospheric disturbances (SID) in the VLF recordings. Daily quiet daily curves provide a baseline from which flare-induced absorption can be calculated. In order to study these SID one needs to subtract the quiet day curve from the recordings (Figure 1). Unfortunately, there are various reactions forming the quiet ionospheric D-region, based on Lyman-α radiation, solar X-ray radiation as well as through the formation of various Ions from atomic oxygen, molecular oxygen, nitrogen and combinations forming nitrogen oxides.

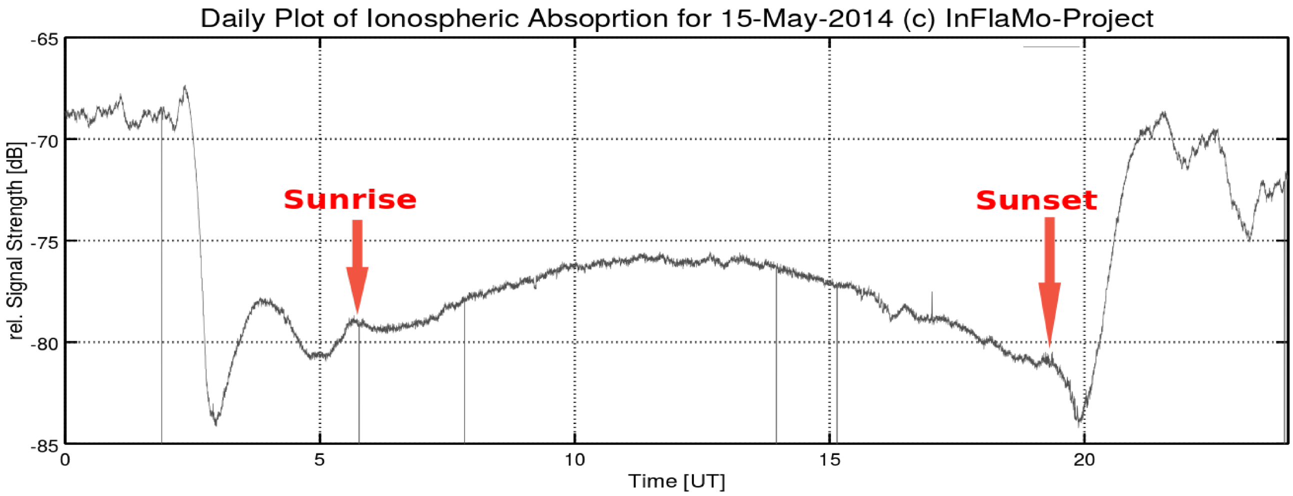

Figure 1: Quiet day curve (QDC) from May 15th, 2014 at 22.1 kHz. Transmitted at Skelton, UK and recorded at Bentzin, Germany. The spikes in the data are caused artificially by sources near by the receiver station. Times for sunrise at the transmitter station and sunset at the receiver station are marked.

Analysis of the Quiet Day Curve and Selected Data

a) The regression method:

The time interval which defines a quiet day curve is given by the time of the sunrise time of the more westward positioned station (transmitter or receiver) and the sunset time at the other station. Several regression methods are applicable for a fitting. Polynomial regression 2nd order provides an easy way to analyze the length of the sunlit condition as well as the relative maximum of signal strength at the mid point (on a great circle) between the both transmitter and receiver stations. A Polynomial regression 8th order provides a most accurate fit for most quiet day curves, but includes too many fitting parameters. Therefore, the approach of a cosine regression from Schumer (2009) was applied for the present study. With the intensity of the signal, I(t), given

$$I(t) = A * \cos^{0.9}(\Theta_t) + B \qquad \text{(eq. 1)}$$

where the parameter, A, is a scaling factor which contains information about ionizing Lyman-α flux, local NO^+ densities, and background solar X-ray flux. The parameter, B, in equation 1 represents the received strength of the VLF signal in the absence of any loss. The power of that dependence, r =0.9, was found consistent with Schumer (2009) and references there-in, which suggested the power of the cosine dependence of D-region absorption at mid-latitudes is between 0.6 and 1.0. The zenith angle, Θ_t, is computed for the coordinate of the mid point of the radio propagation path between transmitter and receiver.

b) The data analysis:

In order to compare quiet day curve behavior at solar maximum and minimum of the solar cycle 24 it is necessary to find corresponding days of the year. For this, a period from April to August 2014 and April to August 2019 was chosen. Figure 2 shows (from top to bottom) the Kp index, sun spot number R, solar radio flux F10.7 and Lyman-α ionizing flux. Note that Kp index representing the geomagnetic activity is similar in the selected periods (marked by light-red boxes in Figure 2) in solar maximum and minimum, whereas the variables showing the solar activity differ, exhibiting the typical variation between solar maximum and minimum.

We found each five days for 24.0 kHz (Cutler, Main, USA) and 22.1 kHz (Skelton, UK), which fulfilled our criteria. The daily F 10.7 fluxes were provided by the courtesy of the National Research Council Canada in partnership with the Natural Resources Canada. To obtain a better understanding of the seasonal behavior four additional days were selected at solar maximum for Cutler, USA.

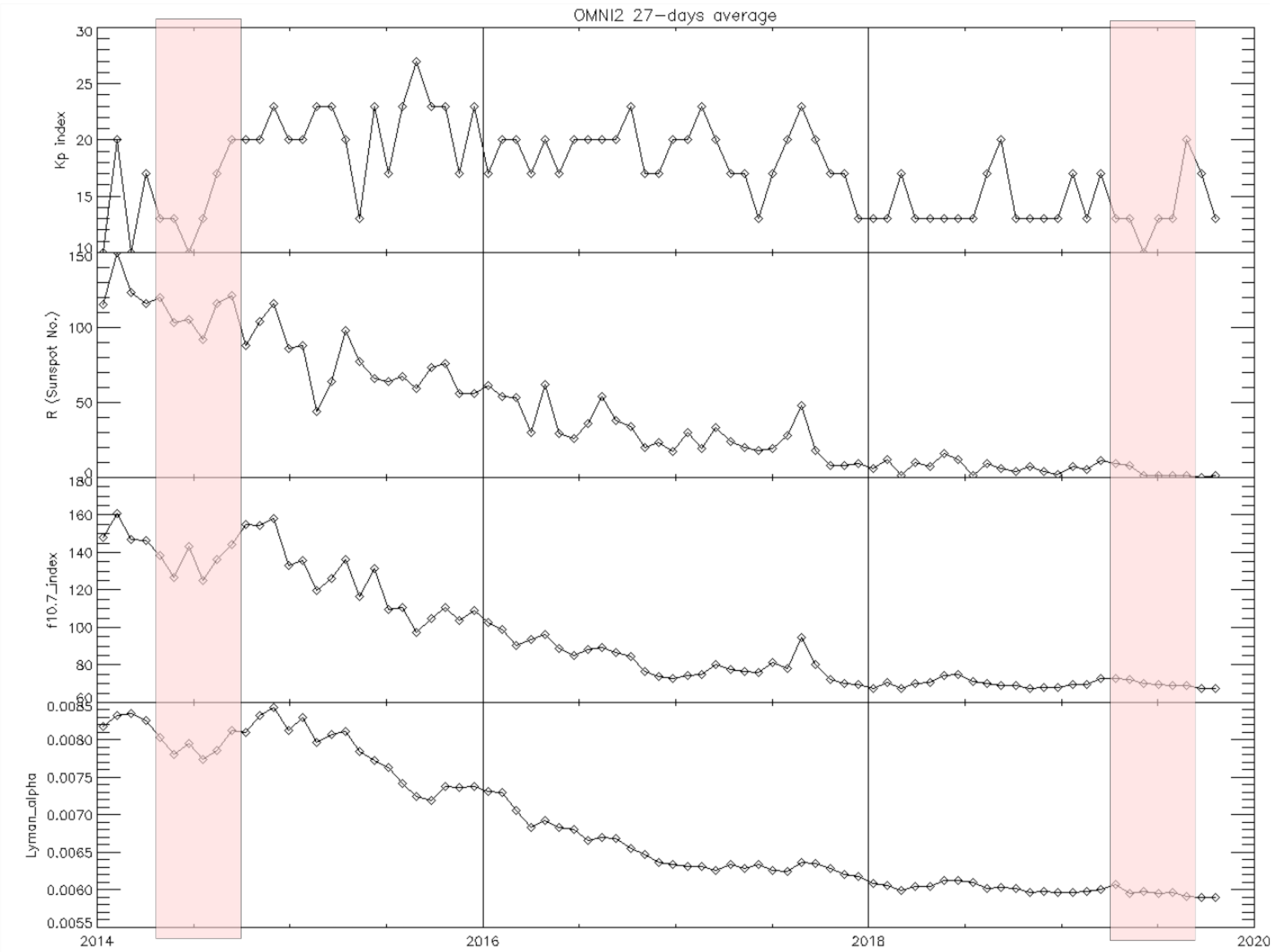

Figure 2: Kp index, sunspot number, F 10.7 radiation flux and Lyman-α flux for the time from solar maximum to minimum of solar cycle 24. The highlighted intervals are marking the time periods used for the present study. Data source: https://omniweb.gsfc.nasa.gov/form/dx1.html

The upper panel of Figure 3 shows a typical quiet day curve. The cosine regression (eq. 1) is computed for all the data points (green line), for which the solar elevation angle (Figure 3, lower panel) exceeds 20°. It was found that for solar elevation angles below 20° the change of ionospheric condition is too rapid to follow the cosine regression. The red line in Figure 3 (upper panel) is the actual regression curve plot onto the data. A good agreement can be seen. The middle panel is the resulting baseline of regression values subtracted from the data points. The parameters A and B from eq. 1 are shown in the headline of the figure.

In this manner all the selected days are processed and the parameters A and B are found. The seasonal variations can be found from the parameter A. Figure 4 shows a that general quadratic regression indicates that the parameter A is lowest in the summer and enhanced at spring and autumn. For the other days and frequency the same behavior is found.

The ratio of values A obtained for solar maximum and minimum for the same days of year are expected to provide inside into the unknown quantity of the ionospheric D-region production. Figure 5 shows those ratios. The linear regression indicates that the values of A are larger during solar maximum than in solar minimum.

The change of received strength of the VLF signal in the absence of any loss during solar maximum and minimum is shown as ratios in Figure 6. With 0.87 inclination and 23.47 offset of the linear regression function one can neglect any major changes of parameter B due to solar cycle variations.

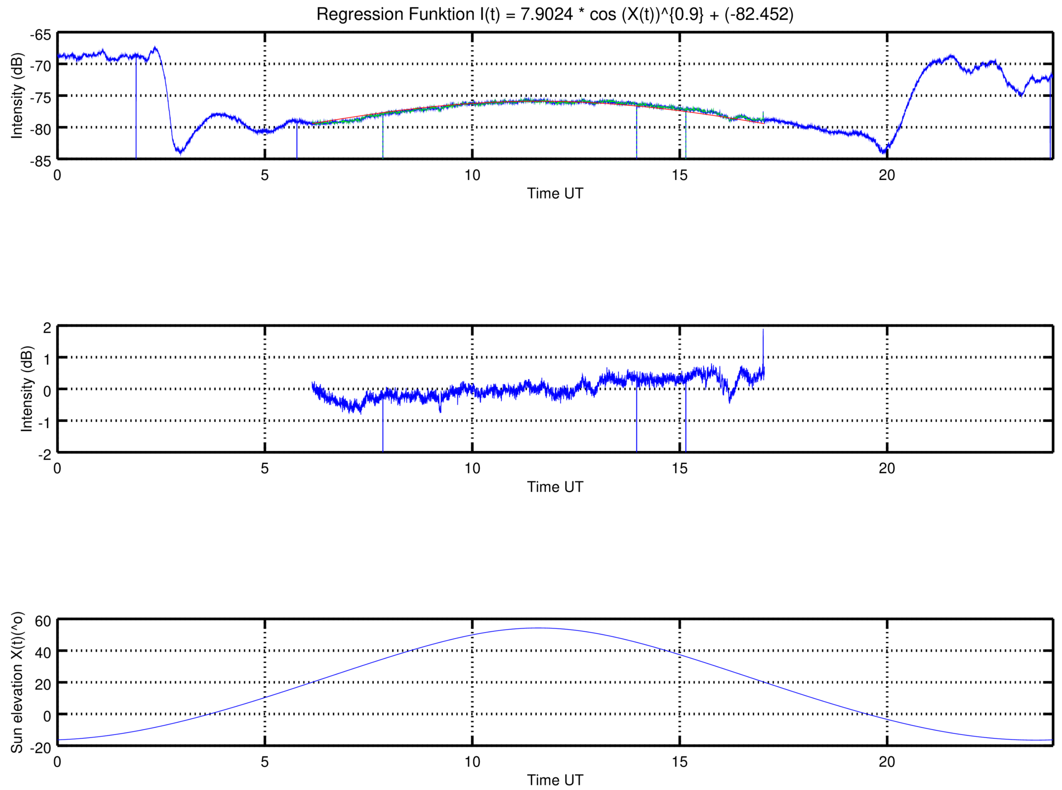

Figure 3: Processing of a quiet data curve. Upper panel: The red line indicates the cosine regression. Middle panel: Resulting baseline of the subtraction of regression function from the data. Lower panel: Sun elevation vs. time.

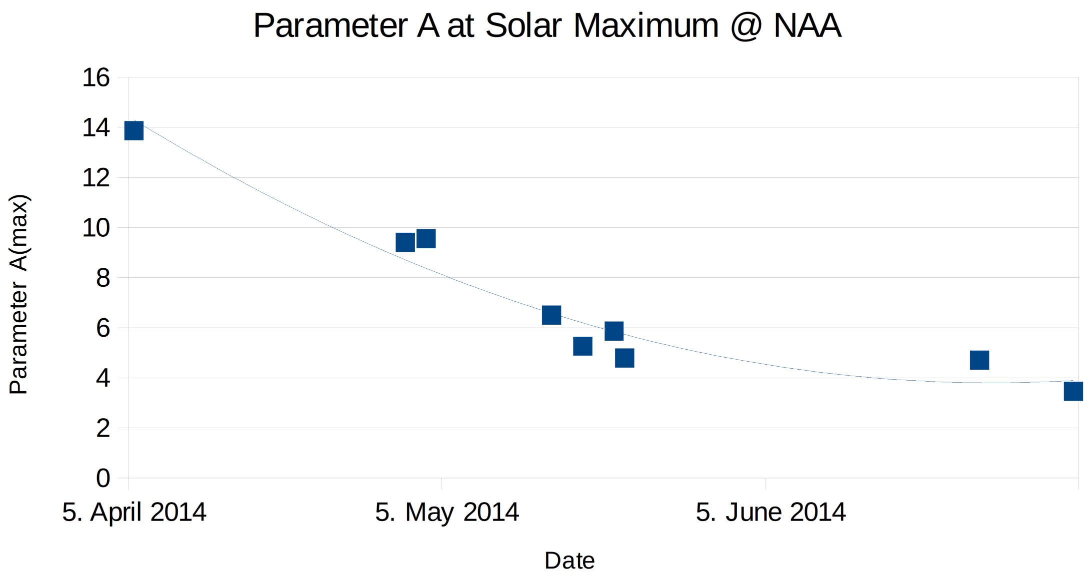

Figure 4: Seasonal dependence of parameter A from eq. 1. The quadratic regression line shows a minimum around mid-summer.

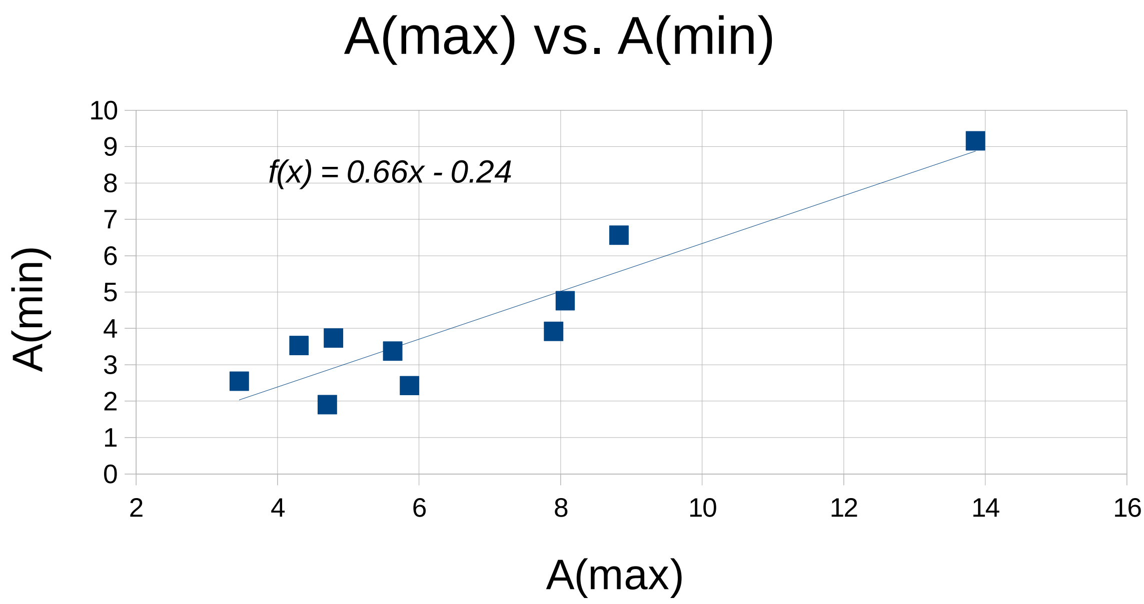

Figure 5: A ratio of parameter A at the same days of year for solar maximum and minimum is shown. A linear regression is shown (blue line).

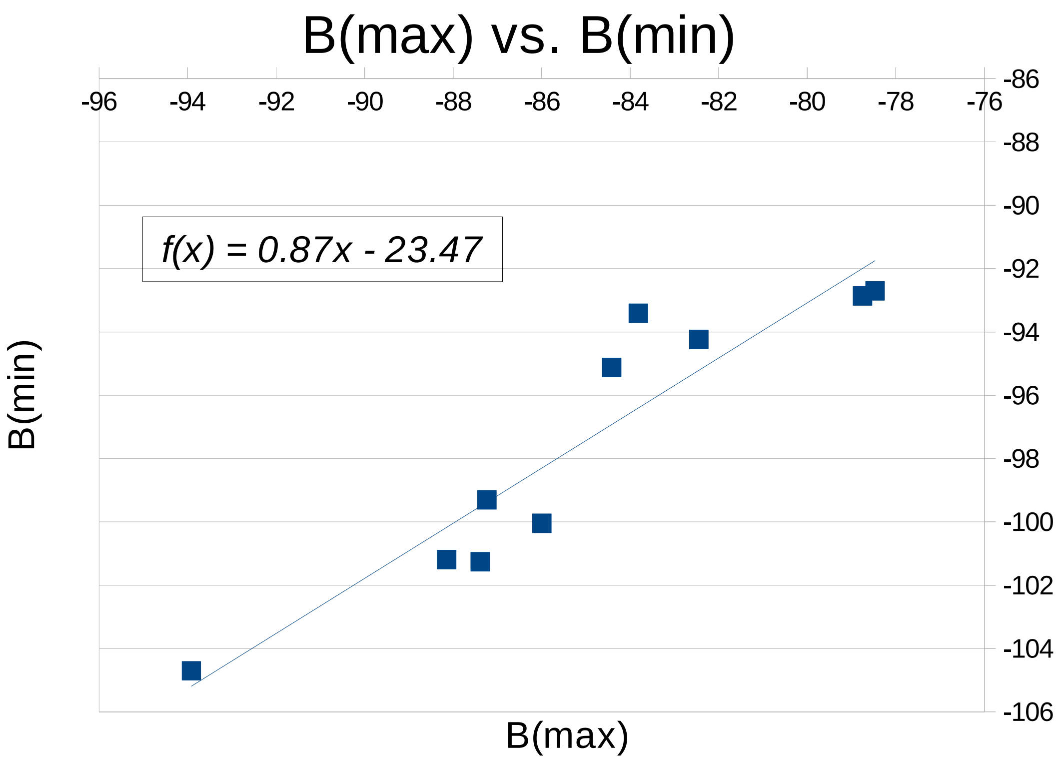

Figure 6: A ratio of parameter B at the same days of year for solar maximum and minimum is shown. The linear regression is shown (blue line).

Figures 7 and 8 are showing the F 10.7 radiation fluxes at selected time periods during solar maximum and minimum. There is no seasonal variation found. As already seen in Figure 2 it is evident that the F 10.7 radiation flux is about doubled during solar maximum compared to solar minimum. The main ionizing flux for NO is solar Lyman-α shown in Figure 2. To ionize N_2 and O_2, X-ray or EUV flux of shorter wavelengths is needed. Though F10.7 radiation flux is not a primary driver for the production of a D-region reflection layer, it is often used as a proxy, especially for investigations over larger time periods.

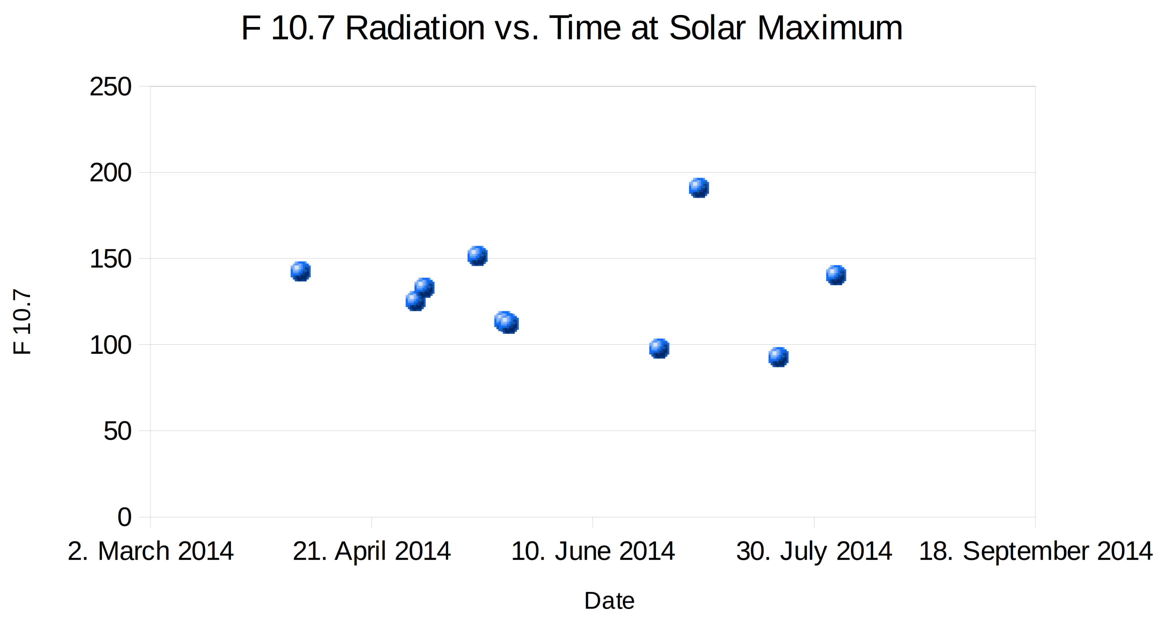

Figure 7: F 10.7 cm flux values is given in sfu = 10^{-22}W m^{-2} Hz^{-1} for the selected time period at solar maximum. These measurements are provided courtesy of the National Research Council Canada

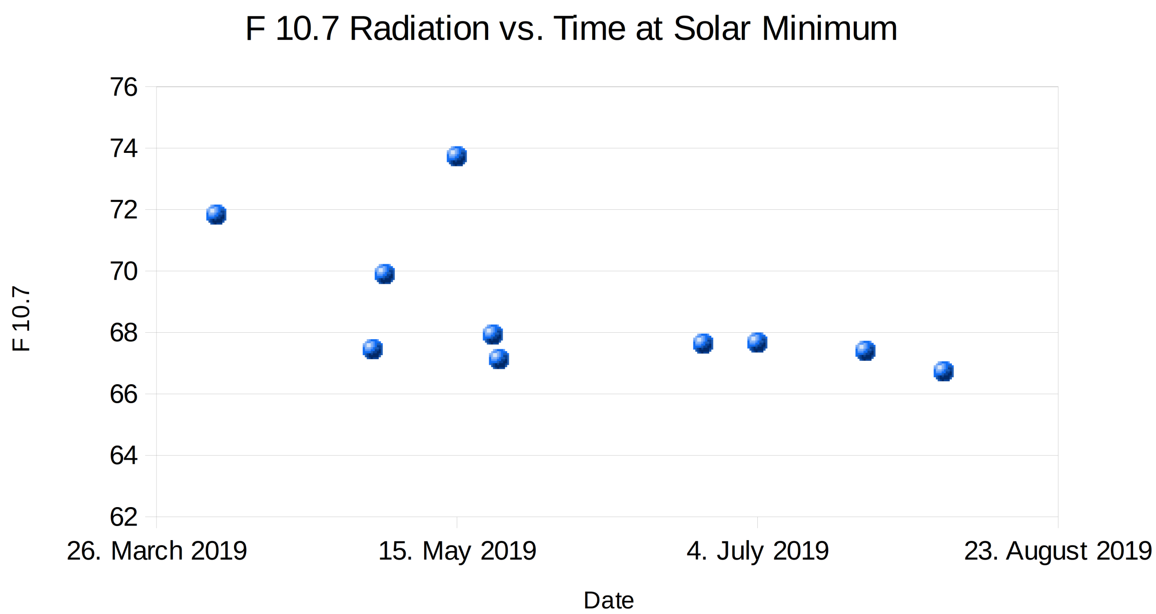

Figure 8: F 10.7 cm flux values for the selected time period at solar minimum. More details see Figure 7.

Discussion and Conclusion

We show that the change of Lyman-α radiation flux had a relatively small variability and its behavior is similar to the F 10.7 radiation flux. The selected days were all calm in respect to solar X-ray radiation. There were no sudden solar X-ray flares observed and the Kp-index is for both time intervals at solar maximum and minimum about the same. It is known (Reid, 1976) that the increase of solar activity leads to an increase in the strength of the solar wind. A strong solar wind is reducing the flux of cosmic rays that can penetrate the inner solar system from outside. In the case of reduced solar activity the galactic cosmic rays can penetrate deeper into the inner solar system, which causes an inverse dependence on solar activity. Reid (1976) found that the production of ions in the D-region can rise up to 25 % during solar minimum due to this effect. In the present study we find a change of parameter A, which combines various production terms, of about one third (Figure 5). The change of received strength of the VLF signal in the absence of any loss during solar maximum and minimum is found to be small (Figure 6) and is not further discussed in content of this preliminary study.

The D-region ionization is the most complex of all the ionospheric layers and strongly dependent on the existence of many minor constituents, which do not exist higher up in the ionosphere. There are mainly nitric oxide and various cluster or more complicated molecular ions and metastable exited species to name.

Other measuring techniques, such as riometer or attenuation of signals from Doppler sounders (Chum et al., 2018) can also provide valuable information about the D-region dynamics. For solar cycle 24 this is not possible. The InFlaMo-Project (http://www.inflamo.org) has been operating a VLF receiver nearby the Doppler sounding radar since summer 2019. For future studies the described cosine regression analysis combined with a multi instrumental setup will be used.

References:

1. Chum J. et al., Continuous Doppler sounding of the ionosphere during solar flares, Earth, Planets, 2018.

2. Hargreaves, J.K., The Solar-Terrestrial Environment, Cambridge University Press, 1992.

3. Pal, S., Chakrabarti, S. K., Theoretical models for Computing VLF wave amplitude and phase and their applications, AIP Conference Proceedings., 1286, 42–60, 2010.

4. Reid, G.C., Ionospheric Effects of Solar Activity, Solar Activity Observations and Predictions, by P.S. McIntosh and M. Dryer. Translated from the English edition. Moskva: Mir., pp.293-312, 1976.

5. Schumer, E.A., Improved modeling of mid-latitude D-region ionospheric absorption of high frequency radio signals during solar X-ray flares, Air Force Institute of Technology, Air University, PHD-Thesis, 2009.